

A bioactive injectable self-healing anti-inflammatory hydrogel with ultralong extracellular vesicles release synergistically enhances motor functional recovery of spinal cord injury

Chenggui Wang^{a,1}, Min Wang^{b,1}, Kaishun Xia^a, Jingkai Wang^a, Feng Cheng^a, Kesi Shi^a, Liwei Ying^a, Chao Yu^a, Haibin Xu^a, Shining Xiao^a, Chengzhen Liang^a, Fangcai Li^{a,***}, Bo Lei^{b,**}, Qixin Chen^{a,*}

^a Department of Orthopedics Surgery, 2nd Affiliated Hospital, School of Medicine, Zhejiang University, Hangzhou, 310009, Zhejiang, PR China

^b Key Laboratory of Shaanxi Province for Craniofacial Precision Medicine Research, College of Stomatology, Frontier Institute of Science and Technology, Xi'an Jiaotong University, Xi'an, 710054, PR China

ARTICLE INFO

Keywords:

Bioactive biomaterials
Multifunctional hydrogel
Extracellular vesicles release
Spinal cord injury repair

ABSTRACT

The repair and motor functional recovery after spinal cord injury (SCI) remains a worldwide challenge. The inflammatory microenvironment is one of main obstacles on inhibiting the recovery of SCI. Using mesenchymal stem cells (MSCs) derived extracellular vesicles to replace MSCs transplantation and mimic cell paracrine secretions provides a potential strategy for microenvironment regulation. However, the effective preservation and controlled release of extracellular vesicles in the injured spinal cord tissue are still not satisfied. Herein, we fabricated an injectable adhesive anti-inflammatory F127-polycitrate-polyethyleneimine hydrogel (FE) with sustainable and long term extracellular vesicle release (FE@EVs) for improving motor functional recovery after SCI. The orthotopic injection of FE@EVs hydrogel could encapsulate extracellular vesicles on the injured spinal cord, thereby synergistically induce efficient integrated regulation through suppressing fibrotic scar formation, reducing inflammatory reaction, promoting remyelination and axonal regeneration. This study showed that combining extracellular vesicles into bioactive multifunctional hydrogel should have great potential in achieving satisfactory locomotor recovery of central nervous system diseases.

1. Introduction

Spinal cord injury (SCI) is a devastating trauma that causes several disabilities and sequelae for individuals [1–3]. Following the primary trauma causing structural disturbance, long-term complications of secondary injury occur around the lesion site comprising inflammation, apoptosis, demyelination and scars tissue formation [4]. Therefore, these intricate microenvironments will limit the effective treatment of SCI [5]. Moreover, it is hardly achieving a satisfactory therapeutic effect with targeting a single parameter. Hence, integrative regulation of the partial microenvironment is a promising therapeutic strategy for SCI [6–8].

Fortunately, the stem cell transplantation therapy for SCI has been evoked much attention as a promising strategy to regulate microenvironment and improve recovery of motor, sensory, and/or autonomic functions [9,10]. Due to the relative ease of acquisition and culture, mesenchymal stromal cells (MSCs) have emerged as promising stem cell sources for regenerative medicine [11]. Moreover, MSCs was demonstrated that it could improve motor functional recovery after SCI via directing neuronal differentiation of progenitor cells, reducing scar tissue formation and enhancing axonal regeneration [12,13]. Although MSCs exhibit a remarkable outcome to promote functional plasticity after spinal cord injury, the direct transplantation of stem cells to target tissues remains limited in clinic. The reasons include the low survival

Peer review under responsibility of KeAi Communications Co., Ltd.

* Corresponding author.

** Corresponding author.

*** Corresponding author.

E-mail addresses: lifangcai@zju.edu.cn (F. Li), rayboo@xjtu.edu.cn (B. Lei), zrcqx@zju.edu.cn (Q. Chen).

¹ These authors contributed equally to this work.

<https://doi.org/10.1016/j.bioactmat.2021.01.029>

Received 19 October 2020; Received in revised form 17 January 2021; Accepted 24 January 2021

2452-199X/© 2021 The Authors. Production and hosting by Elsevier B.V. on behalf of KeAi Communications Co., Ltd. This is an open access article under the CC

BY-NC-ND license (<http://creativecommons.org/licenses/by-nc-nd/4.0/>).

rate of transplanted stem cells, the inevitable immune rejection and possible cell dedifferentiation/tumor formation [14–20]. Transplanted stem cells exert therapeutic effects mainly through important bioactive molecules, which are mediated by paracrine action primarily after transplantation [15,16]. Extracellular vesicles, a principal form of paracrine secretory ingredients, have been confirmed that they could regulate cell-to-cell communications through transferring the contained mRNAs, miRNAs, and proteins to target cells. Hence, it is hypothesized that MSCs-derived extracellular vesicles could perform the similar benefit functions as MSCs in therapy of spinal cord injury.

However, the challenges containing short half-time and rapid clearance due to the innate immune system will become an obstacle for extracellular vesicles therapeutics [17]. Furthermore, MSCs-derived extracellular vesicles have been manifested that it could alleviate the local SCI microenvironment, while the poor accumulation in the spinal cord lesion site after systemic administration greatly decreased the efficiency due to the rapid clearance *in vivo* [18–20]. Additionally, the recovery process of spinal cord commonly experiences a complex and lengthy multiple phase, it is difficult to retain the unconjugated or free extracellular vesicles in the injured site for an extended time [21]. Herein, it is necessary to develop an innovative and biocompatible biomaterial vehicle that can serve as a sustained release carrier for extracellular vesicles, exhibiting efficient retention and sustained release at the spinal cord injured area and further accelerate axonal regeneration.

In recent years, biomedical hydrogels have gained treatment interest in drug/cell delivery applications due to 1) exhibiting an obvious three-dimensional porous morphology, which provides a certain load space for the delivery bioactive factors or cells; 2) having multifunctional properties including thermosensitivity, injectability, self-healing ability and adhesive, which facilitates the *in vivo* applications; 3) showing a good cytocompatibility based on the rational design to ensure the good survival of cells and effective release of bioactive factors [22–24]. Although plenty of hydrogels have been used in extracellular vesicle delivery, their further application for repairing SCI remains limited due to the lack of multifunctional properties, inherent bioactivity and long term release [25]. As the advantages of facile synthesis, high biocompatibility, controllable biodegradation and low cost, citric acid-based polymers (CABP) have attracted widespread attention in tissue engineering [26]. To expand the applications, our group developed multifunctional citric acid-based polymers, which preformed sensational biomedical effects in bioimaging, nucleic acid delivery and tissue regeneration [26–28]. Interestingly, we found that polycitrate-polyethylene glycol-polyethyleneimine (PCE) performed excellent biocompatibility. Moreover, it can promote cell activities in skeletal muscle regeneration [29]. It is very promising to design a PCE-based hydrogel with multifunctional properties and long term local release of MSC-derived extracellular vesicle for efficient treatment of SCI.

Herein, a thermosensitive and injectable adhesive anti-inflammatory PCE-based hydrogel (FE) with locally sustainable and stable delivery for extracellular vesicle was designed for treating SCI. The FE hydrogel was prepared through a dynamic hydrogen bond between F127 and PCE polymer, the MSC-derived extracellular vesicle was loaded by the electrostatic interaction with PCE. The multifunctional properties of hydrogels including injectability, adhesiveness, temperature-responsive and self-healing were evaluated. The synergistic effects of local long term release of extracellular vesicle and FE hydrogel on the anti-inflammatory activity, pathology and motor function, fibrotic scar tissue formation, remyelination and axonal regeneration were investigated in detail.

2. Results

2.1. Ad-MSCs and exosomes characterization

The obtained Ad-MSCs were characterized by osteogenic, and

adipocyte differentiation assay based on Alizarin red and Oil Red O staining, respectively. We found that they have osteogenic and adipocyte differentiation ability (Fig. S1A). Passage 4–5 of Ad-MSCs were assessed for flow cytometry analysis. They were found to negative expression of CD34, and CD45 and HLA-DR, positive expression of CD73 (Fig. S1B). The presence of CD63, CD81, Alix and TSG101 expression in the extracellular vesicles was confirmed by western blot (Fig. S1C). Furthermore, the result of immunofluorescence showed that PKH67 labeled extracellular vesicles were localized in neurons (Fig. S1D) after cultured for 24 h, suggesting that extracellular vesicles could be endocytosed by neurons. The spherical extracellular vesicle morphology was confirmed by transmission electron microscopy (TEM) (Fig. S1E). Meanwhile, the concentration and size distribution of the extracellular vesicle was about 50–200 nm measured by ZetaView (Fig. S1F), which was concordant with the previously reported [30]. Taken together, these results showed that the isolation and purification of Ad-MSCs derived extracellular vesicles were successful, which performed endocytosis and bioactivity in neurons.

2.2. Fabrication and characterizations of FE and FE@EVs hydrogel

The temperature-responsive FE hydrogel was prepared using F127 and PCE through the hydrogen bond, and then the extracellular vesicles were encapsulated by electrostatic interaction with PCE in hydrogel. During the treatment of SCI, the local long-term release of extracellular vesicles and PCE possessed a certain anti-inflammatory activity, reduction of fibrotic scar, remyelination and improvement of axonal regeneration. The PCE polymer was synthesized through a two-step chemical reaction (Fig. S2). The chemical structure of PCE polymer was determined by ^1H NMR analysis (Fig. 1A). The peaks between 2.27 ppm and 3.09 ppm were assigned to the methylene ($-\text{CH}_2-$) of CA and PEI. The peaks around 3.60 ppm were attributed to the methylene ($-\text{CH}_2-$) of PEG. The peaks at 1.24 ppm and 1.54 ppm were identified as the methylene ($-\text{CH}_2-$) of OD. The peaks between 3.84 ppm and 4.31 ppm was belonged to the methylene ($-\text{COO}-\text{CH}_2-$) connected to the ester bond. The peaks between 3.10 and 3.30 ppm was belonged to methylene ($-\text{CONH}-\text{CH}_2-$) connected to amido bond. The presence of new peaks indicated the successful synthesis of PCE polymer. The ^1H NMR spectra of raw materials including citric acid (CA), 1,8-octanediol (OD), PEG, PCG prepolymer and PEI was shown in Fig. S3. The chemical structure of PCE polymer and FE hydrogel were also analyzed by FTIR spectra (Fig. 1B). The broad peaks between 3700 cm^{-1} and 3200 cm^{-1} were attributed to the hydroxyl ($-\text{OH}$) of diols and the amino of PEI. The peaks between 3000 cm^{-1} and 2750 cm^{-1} were assigned to the methylene ($-\text{CH}_2-$) of CA, OD, PEG and PEI. The presence of peaks between 1800 cm^{-1} and 1650 cm^{-1} belonged to the ester bonds ($-\text{COO}-$) and amido bond ($-\text{CONH}-$) further indicated the successful synthesis of PCE polymer. The FTIR of F127 and FE hydrogel has been shown in Fig. S4. The peak at 1100 cm^{-1} belonged to the ether bond ($-\text{C}-\text{O}-\text{C}-$) from F127. The characteristic peak of PCE was not obvious due to the low content of PCE (0.01%) in FE hydrogel. It was detected by selecting the FE' hydrogel containing high concentration of PCE (2.5%). The appearance of above-mentioned peaks indicated that FE hydrogel was successfully formed. In addition, the more obvious 3D porous morphology of FE@EVs hydrogel was observed by SEM (Fig. 1C).

The multifunctional properties and rheological properties of the hydrogel are shown in Fig. 1. The FE@EVs hydrogel exhibited the sol to gel transition temperature above $25\text{ }^\circ\text{C}$, indicating its thermosensitivity (Fig. 1D). The FE@EVs hydrogel could be extruded from the $0.9\times 38\text{ mm}$ needle without obstruction to form “FFE” shape, suggesting its good injectability (Fig. 1E). After approximately 1 h, the two pieces of FE@EVs hydrogel could be able to heal together, suggesting the FE hydrogel possesses certain self-healing ability due to the existence of the hydrogen bond (Fig. 1F). In addition, the FE@EVs hydrogel can allow the two spinal cords or skin to adhere together without dropping, suggesting its good adhesive ability (Fig. 1G). The rheological properties

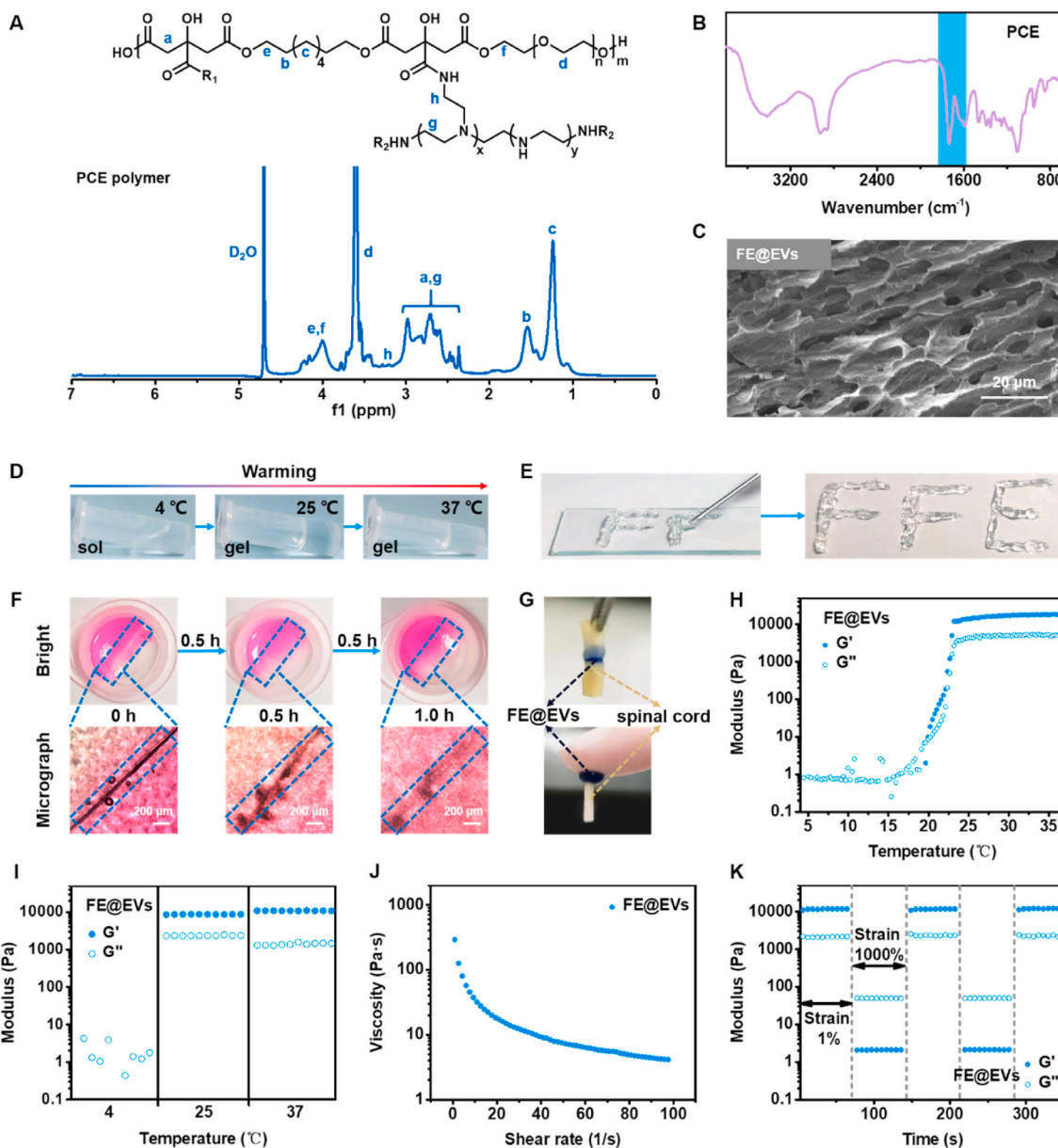


Fig. 1. Physicochemical structure and multifunctional properties of FE@EVs hydrogel. (A) ^1H NMR spectra of PCE polymer; (B) FTIR spectra of FE hydrogel. (C) SEM image of FE@EVs hydrogel. (D) The sol-gel transition of FE@EVs hydrogel with temperature changes. (E) The photographs of FE@EVs hydrogel through the needle. (F) The photographs of FE@EVs hydrogel placed for a while after being cut off. (G) The photographs of FE@EVs hydrogel adhering to spinal cord. (H) The G' and G'' changes of FE@EVs hydrogel at 4 °C–38 °C; (I) The G' and G'' of FE@EVs hydrogel at 4, 25 and 37 °C within 1 min; (J) The viscosity changes of FE@EVs hydrogel at 1 1/s to 100 1/s shear rate. (K) The G' and G'' changes of FE@EVs hydrogel after two cycles of step strain.

were also measured to evaluate the mechanical behavior of the hydrogel. The storage modulus (G') gradually exceeded the loss modulus (G'') of FE@EVs hydrogel when the temperature gradually increased from 4 °C to 37 °C, indicating the sol-gel transformation (Fig. 1H). The G' and G'' of FE@EVs hydrogel also exhibited a certain stability at 25 °C and 37 °C (Fig. 1I). At the shear rate changed from 1 to 100 1/s, the viscosity of FE@EVs hydrogel gradually decreased from ~ 291 to ~ 4 Pa s, further indicating the injectability of FE@EVs hydrogel (Fig. 1J). After two cycles of step strain (1%-1000%-1%), the modulus (G' and G'') of the hydrogel showed a negligible change, suggesting its good self-healing (Fig. 1K). In addition, F127 and FE hydrogel exhibited the similar mechanical behavior compared with the FE@EVs hydrogel (Figs. S5A–S5D). The above results indicated that FE@EVs hydrogel possessed multifunctional properties including thermosensitivity, injectability, self-healing ability and adhesive to enable its promising

application in injured spinal cord repair.

2.3. The *in vivo* biocompatibility of FE@EVs hydrogel

In order to evaluate the biocompatibility of the FE or FE@EVs hydrogel, the change in body weight was measured at the 7, 14, 21, 28, 35, 42, 49 and 56 days after SCI. All rats lost weight during the first week post-operation, and increased smoothly in a time-dependent manner (Fig. S6A). After 42 days, the FE@EVs treated group gained weight to a greater extent than the SCI group, suggesting that FE@EVs were biological safety and a better locomotion might be attributable to easier food. Furthermore, the H&E staining of the major organs, including heart, liver, spleen, lung and kidney collected from each group was conducted, and there were no obvious changes or any pathologic changes in all major organs harvested from the FE and FE@EVs groups,

further confirming the biocompatibility (Fig. S6B).

2.4. Long term retention and controlled release of extracellular vesicles in FE@EVs hydrogel

The release kinetics of extracellular vesicles by FE hydrogel was performed *in vitro* and *in vivo*. For *in vitro* release profile, an initial burst release (~20%) of extracellular vesicles from FE@EVs hydrogel was observed on first week, and continued cumulative release over ~60% after the following 28 d. Moreover, approximately 89% and 93% of the loaded extracellular vesicles were released from the FE@EVs hydrogel at day 49 and 56, suggesting the sustained long term release (Fig. S6C). To validate the efficient retention and sustained release of extracellular vesicle in FE@EVs hydrogel *in vivo*, the DiR labeled extracellular vesicles-loaded FE hydrogel were injected orthotopically to a spinal cord post-surgery. Besides, DiR labeled extracellular vesicles solution was injected as a control group. As a result, the plummeting fluorescence signal of extracellular vesicles could be observed before 14 days followed by a gentle decrease after 14 days in the control group, indicating that the solution of extracellular vesicles could not retain extracellular vesicles in the injured area. On the contrary, a mild decrease of extracellular vesicles was measured before 28 days followed by a sharply decrease after 28 days in the FE@EVs group (Fig. 2A and B). Compared with the extracellular vesicle solution, FE hydrogel could localize the extracellular vesicles in the SCI site by its good adhesive action with tissue, showing a sustainable and stable controlled release. The *ex vivo* results further showed that the spinal cord tissue in FE@EVs group have stronger fluorescence signal than control group after 56 days (Fig. 2C and D). In addition to the spinal cord, we also detected the fluorescence signal in major organs and the DiR signal was dominantly distributed in kidney, indicating a kidney-mediated excretion of DiR labeled extracellular vesicles (Fig. 2E).

2.5. Improved pathology and motor function after SCI by FE@EVs hydrogel

The effects of FE@EVs hydrogels in promoting motor functional recovery were assessed by BBB locomotion score and footprint analyses. As the spinal cord injury progresses, the animal exhibits flaccid paralysis and then recovers appropriately with the extension of recovery time. The scores in the group of rats that received the treatment of free extracellular vesicles and FE@EVs increased significantly compared with the SCI group after 21 days, however, no significant difference was found between the FE@EVs hydrogel group and extracellular vesicles group before 35 days (Fig. 3A). Interestingly, after 35 days, the significantly high scores in FE@EVs group were observed compared with all other groups; moreover, extracellular vesicles treated group and FE hydrogel group showed remarkable difference after 49 days. The footprint test intuitively revealed a fairly consistent posterior limbs (blue ink) partly coordination and a few stumbled walking trajectories (yellow arrow pointed) at 56 days after SCI in FE@EVs treated group (Fig. 3B). Meanwhile, FE hydrogel and free extracellular vesicles treated animals showed incongruous walking trajectories with extensive dragging but the ankle, knee, hip joint of posterior limbs could significantly move compared with the SCI group showing as the width of blue ink streaks increased (Fig. 3B). Similar with the BBB scores recorded at 56 days, it was showed that rats in FE@EVs group exerted intermittent or claw palm load-bearing support. The histological morphology and the cavity area in the injured spinal cord was measured by H&E staining at 28 and 56 days respectively after SCI (Fig. 3C). Severely damaged tissue and an obvious cystic cavitation was observed on the injured spinal cords at 28 and 56 days after SCI. The relative area of damaged spinal cords in FE@EVs (~32.0%) hydrogel group was significantly small as compared to FE (~68.9% of SCI group in 28 days sections) and free extracellular vesicles (~56.3%), as indicated by smaller lesion areas and less damaged tissue. Moreover, the relative area of cystic cavitation in

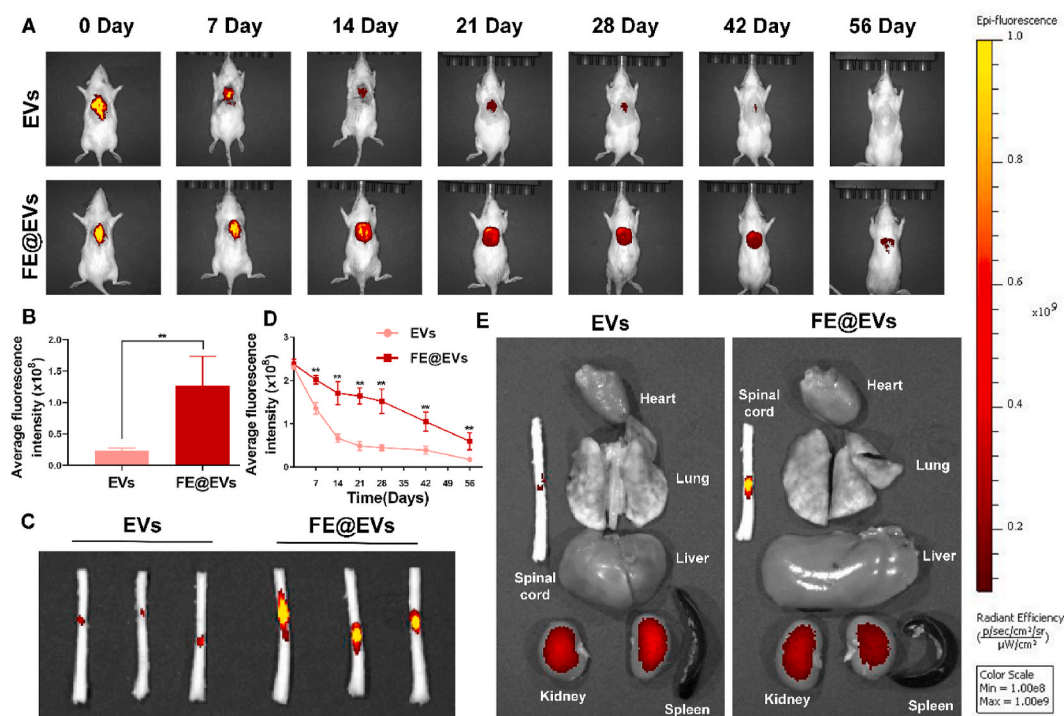


Fig. 2. FE hydrogel improved extracellular vesicles retention. (A, B) Fluorescence image and quantitative analysis of spinal cord extracellular vesicles labeled with DiR between free extracellular vesicles solution and FE@EVs hydrogel group measured using IVIS. (C) Ex vivo spinal cord retention of extracellular vesicles between free extracellular vesicles solution and FE@EVs hydrogel group at 56 days postinjury measured using IVIS. (D) Quantitative analysis of C. (E) Ex vivo retention of extracellular vesicles in major organs between free extracellular vesicles solution and FE@EVs hydrogel group at 56 days postinjury measured using IVIS. N = 4 per group for IVIS.

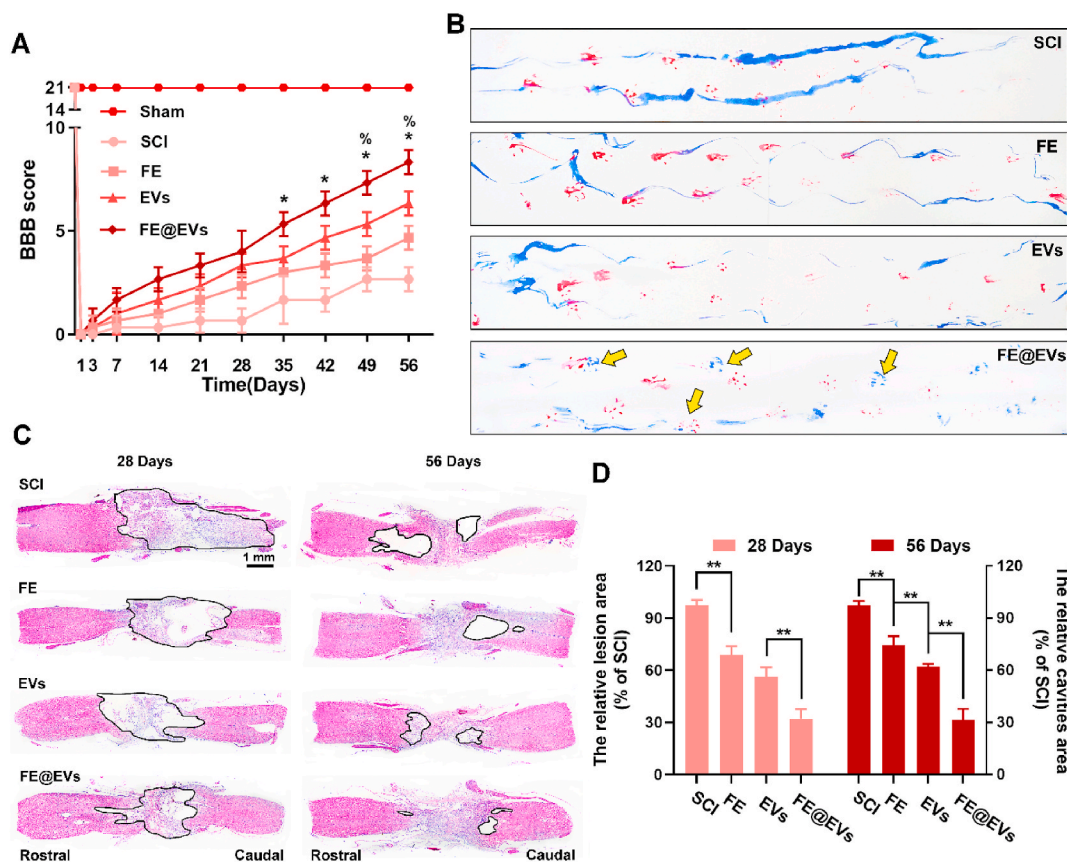


Fig. 3. FE@EVs hydrogel enhance motor function and suppresses the cavity formation after SCI. (A, B) The behavior assay of BBB scores and footprint assay (at 56 days postinjury, yellow arrow pointed the posterior limb prints); * $P < 0.05$ indicate FE@EVs versus EVs group, % $P < 0.05$ indicate FE versus EVs group. (C) H&E staining images of longitudinal sections at 28 and 56 days postinjury. (D) The lesion site area and the cavity area were quantified according to the H&E staining. $N \geq 8$ per group for BBB score and footprint assay, $N \geq 4$ per group for H&E staining at 28 days and 56 days postinjury. (For interpretation of the references to color in this figure legend, the reader is referred to the Web version of this article.)

treated with FE@EVs (~31.6%) hydrogel was also significantly lower than FE hydrogel (~74.4% of SCI group in 56 days sections) and free extracellular vesicles (~62.1%) (Fig. 3D). These results demonstrated that FE hydrogel and extracellular vesicle could synergistically improve pathology and motor function after SCI.

2.6. Reduced fibrotic scar formation and inflammatory reaction by FE@EVs hydrogel

Fibrotic scar in injured spinal cord was detected by the immunofluorescence (Fig. 4A). The results showed that the laminin positive area significantly decreased accompanied by reducing the cavity of lesion site in FE@EVs treated group at 56 days post-injury, as compared to FE hydrogel and free extracellular vesicles treated groups (Fig. 4B). In addition, fibrotic scar related proteins composing NG-2, neurocan and laminin was confirmed by western blot (Fig. 4C–F). Furthermore, the ability of migration of fibroblast affected by FE hydrogel, free extracellular vesicles and FE@EVs were evaluated by a scratch assay. As illustrated in Fig. 4G, the wound area of FE@EVs treatment group was remarkably decreased approximately 85.0% and 37.4% at 24 h and 48 h respectively compared with control group (about 35.4% and 11.6%). Additionally, fibroblast exerted a mild migration rate in FE hydrogel and free extracellular vesicles treated group, while still faster than FE@EVs treated group (Fig. 4H). Specifically, the transwell assay results were consisted with the scratch assay, which showed the significantly decreased migration ability of fibroblast after FE@EVs treatment (Fig. 4G and I).

To show the effect of hydrogels on the inflammatory reaction, the

quantity and distribution of activated macrophages were analyzed by CD68 and Iba-1 immunofluorescence staining. Abundant CD68 positive macrophages were centralized in the injured site and the damaged boundary after SCI (Fig. 5A). While FE@EVs treatment markedly reduced the number of activated macrophages in the injured site as well as limited them infiltrating and presented them almost exclusively in the injured margin (Fig. 5B–E) [31,32]. In addition, FE hydrogel and free extracellular vesicles treated groups performed suppressing macrophages activation as well, however, the effect was still lower than FE@EVs treated group. The reason was probably that FE hydrogel showed a remarkable adhesive property, which could protect the integrity of the injured spinal cord and promote blood-brain spinal cord barrier recovery [33]. Moreover, FE@EVs showed the sustainable and stable controlled release of extracellular vesicles, which enhanced the free extracellular vesicle location in the injured site of spinal cord. Furthermore, western blot assay of CD68 and Iba-1 confirmed the markers of activated macrophages or microglia (Fig. 5F–H). Our *in vitro* study showed LPS stimulated microglia manifested a remarkable activation by Iba-1 staining, meanwhile it reversed by FE@EVs treatment which consist with *in vivo* experiments (Fig. 5I and J).

2.7. Promoted remyelination and axonal generation and reduced neurons apoptosis after SCI

LFB staining was used to verify the degree of myelin sheath destruction and evaluate the effect of the FE@EVs on remyelination. The total area of LFB positive myelin significantly increased in FE@EVs treated group compared with FE and extracellular vesicle and SCI group

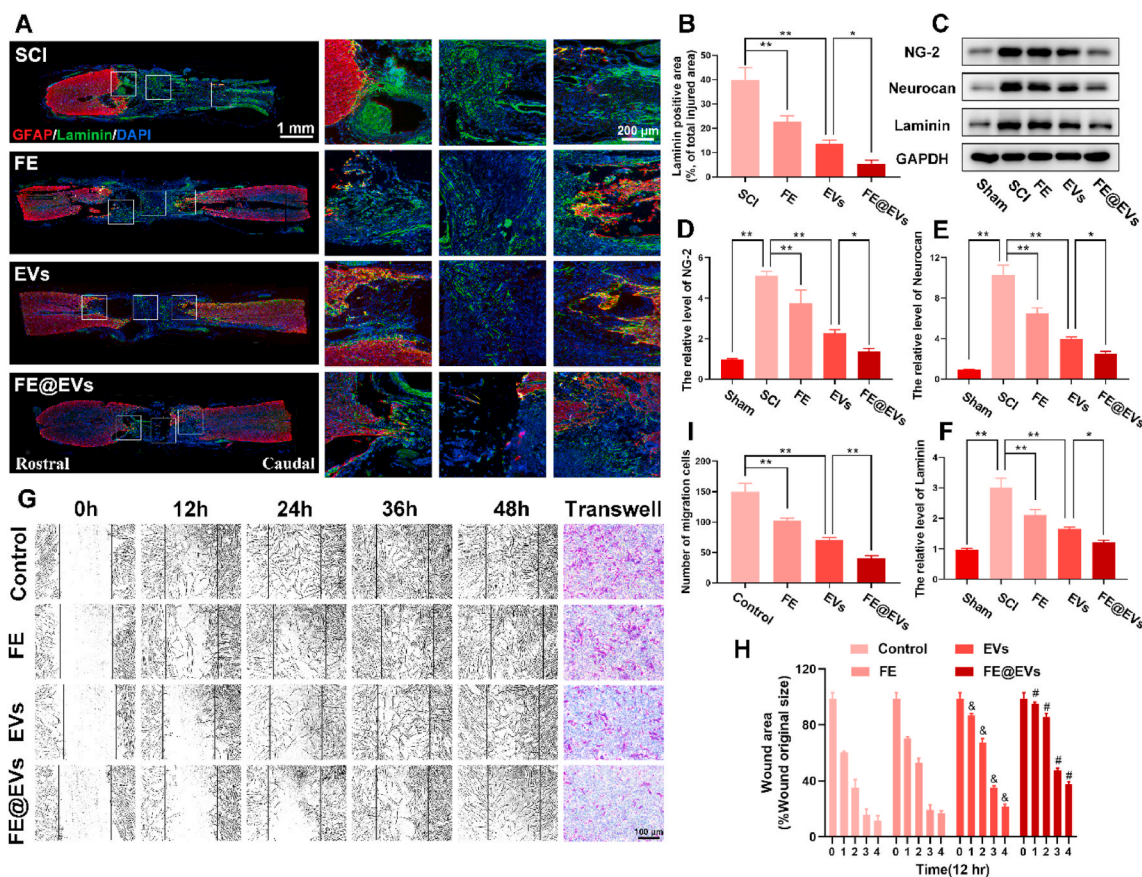


Fig. 4. Fibrotic scar tissue was inhibited by FE@EVs hydrogel. (A) Images of spinal sections staining laminin and GFAP from SCI and different treatment rats at 56 days postinjury. (B) Quantification of laminin positive area in the lesion site. (C–F) Representative western blotting images and quantification showing NG-2, Neurocan and Laminin protein levels in the lesion region. (G, H) Images and quantification migration of fibroblast treated in different groups; $^{\&P} < 0.05$ versus the control group, $^{\#P} < 0.05$ versus the control group. (I) Quantification data of fibroblast migrated from the transwell assay of G. $N \geq 4$ per group for histology analysis, $N \geq 4$ per group for western blot assay.

(Fig. 6A and B). Meanwhile, the transmission electron microscope (TEM) was utilized to evaluate the microstructure of myelin. The distinct and evident effect on myelin sheath restoration was observed after FE@EVs treatment, which showed mildly clear and closely packed layers with abundant microtubules in the axon. The extent of myelin sheath destruction was decreased in FE or free extracellular vesicles treated groups compared with SCI group presenting vacuolar changes, acantholysis and a loss of microtubules (Fig. 6A). Moreover, western blot results were consistent with the immunofluorescence of MBP, indicating that FE@EVs treated group remarkably increased MBP protein expression, presenting a remarkable effect of remyelination (Fig. 6C and D). Additionally, the MBP positive myelin noticeably increased even across the lesion site in FE@EVs treated group (Fig. 6E), suggesting that it manifests an obvious and pronounced effect on remyelination. Besides, FE hydrogel and free extracellular vesicles groups showed a moderate influence on reducing demyelination compared with SCI group (Fig. 6F).

To assay the capacity of axonal regeneration by regulating micro-environment, immunofluorescence and western blot were performed. A structural protein and a constituent of axon microtubules named MAP-2 was detected by immunofluorescence in the injured spinal cord (Fig. 7A). Notably, the distance from neurons (MAP-2 positive cells) to the injury epicenter (white dash line) significantly decreased and effectively prevented robust loss of neurons in FE@EVs treatment group compared with FE and extracellular vesicle group (Fig. 7A and B), suggesting that FE@EVs could distinctly promote axonal regeneration. Additionally, the extension of neurofilaments in the injured spinal cord was detected by immunofluorescence staining of NF-200, which could

further evaluate the axonal regeneration. FE@EVs treated group significantly boost neurofilaments regeneration manifesting punctiform or tubules compared with other groups (Fig. 7C and D). Moreover, the stronger axonal regeneration ability in FE@EVs treated group was also confirmed by the neurofilaments traversing the barrier of glial scar, and the NF-200 and MAP-2 protein expression (Fig. 7E–G). Furthermore, neuronal apoptosis was reduced by FE@EVs treatment, which was indicated by MAP-2 and Bcl-XL immunofluorescence staining (Fig. 7H and I). It was illustrated that FE@EVs could reverse the TBHP-induced neuronal apoptosis and promote axonal regeneration, as compared to other groups. The expressions of Bax, cleaved-caspase-3 and cytochrome c were proportional to the level of neuronal apoptosis, which was opposite to the immunofluorescence of MAP-2 and Bcl-XL (Fig. 7J–N).

3. Discussion

In this study, we developed an injectable, adhesive and anti-inflammatory hydrogel with consistent release of extracellular vesicles after spinal cord injury for effectively promoting functional repair and locomotor recovery. FE@EVs hydrogel exerted efficient comprehensive mitigation microenvironment and set up favorable terms for functional restoration after SCI, through enhancing remyelination, reducing inflammatory reaction, suppressing fibrotic scar formation and promoting axonal regeneration.

Recently, mass of studies has demonstrated that the systemic administration of MSCs-derived extracellular vesicles could attenuate apoptosis, inflammation and enhance functional motor or sensory recovery after SCI [18–20]. In addition, the multi-dose regimen of

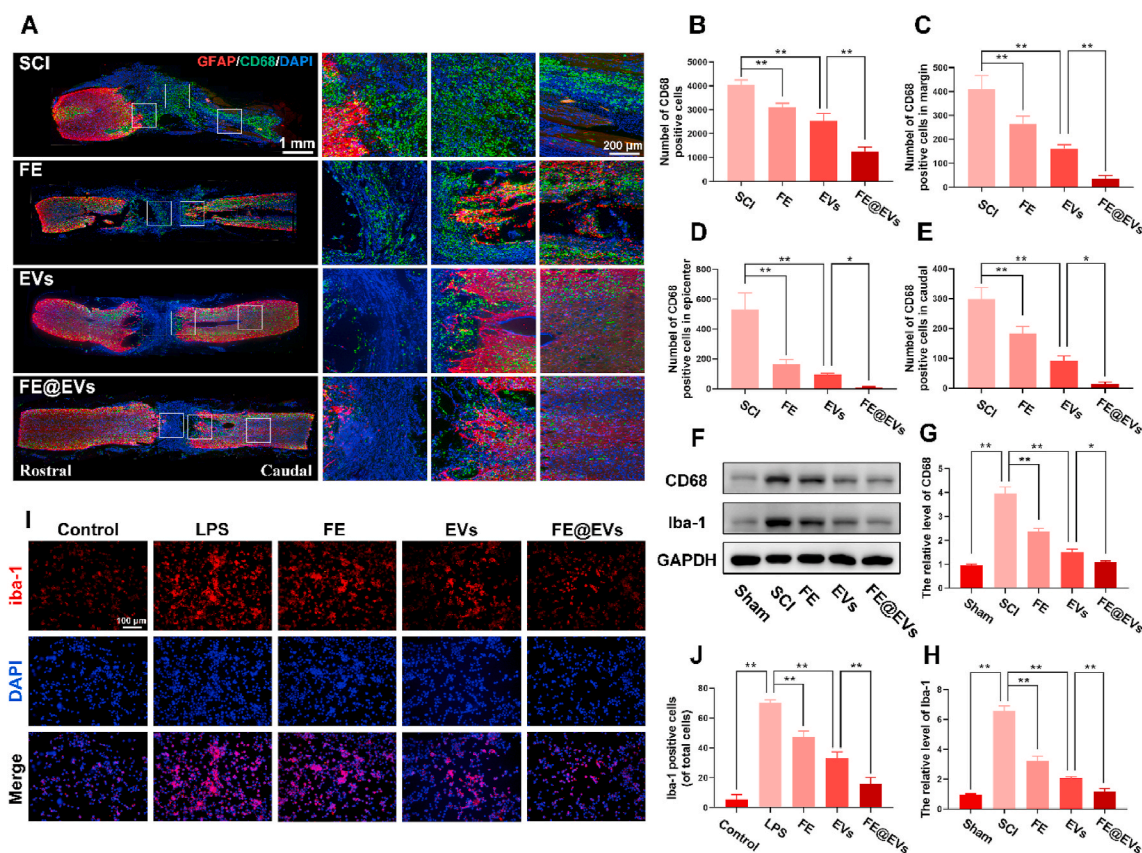


Fig. 5. FE@EVs hydrogel reduces inflammatory reaction. (A, B) Images and quantification of whole spinal sections staining CD68 and GFAP from SCI and different treatment rats at 56 days postinjury. (C–E) The number of CD68 positive cells in epicenter, margin and caudal of spinal cord. (F–H) Protein expressions of CD68 and Iba-1 in each group. (I) Iba-1 immunolabeling of microglia *in vitro*. (J) Quantification of Iba-1 positive microglia from I. $N \geq 4$ per group for histology analysis, $N \geq 4$ per group for western blot assay.

extracellular vesicles has been proven to be superior in improving tissue regeneration [34], indicating that the therapeutic functions of extracellular vesicles were associated with the dosage. However, the rapid clearance and poor accumulation of free extracellular vesicles in lesion site will reduce its functional bioactivity. In our study, we focused on a multifunctional FE hydrogel to improve the therapeutic effect of extracellular vesicles through retaining it in the injured site and sustained controlled release after administration *in vivo*. As compared to reported bioactive hydrogels, there were several advantages for FE hydrogel. Firstly, FE hydrogel exhibited an obvious 3D porous morphology and possessed a certain positive charge, which provided a certain load space and electrostatic interaction for extracellular vesicles. Secondly, FE hydrogel had multifunctional properties including thermosensitivity, injectability, self-healing ability and adhesive, which provided a good property for injured spinal cord. Thirdly, Both FE hydrogel and its degradation products showed a good cytocompatibility to ensure the good survival of cells. Finally, the FE hydrogel could efficiently loading and enable the local long-term release of extracellular vesicles (56 days), which was very promising to deliver MSCs-derived extracellular vesicles into site of SCI. MSCs-derived extracellular vesicles could intervene the process of secondary injury after SCI to enhance the recovery of motor function [20,35,36].

The treatment strategies for spinal cord injury mainly focus on regulating the local microenvironment, including attenuating excessive inflammatory response [37], promoting remyelination [38], reducing fibrotic scars formation [39] and enhancing regeneration of axons [40]. Thus, multiple integrated evidence *in vivo* were performed to evaluate neural motor recovery after SCI in our study, including functional measurements, pathological and immunofluorescence staining. Extracellular vesicles group showed comparable motor functional recovery on

the basis of BBB score at 28th days after spinal cord injury compared to FE@EVs treated group. Subsequently, the BBB score of FE@EVs group began to recover fast and showed remarkable strengths than extracellular vesicles group after 35 days. For extracellular vesicles treated group, the motor functional recovery already began at the first month after SCI and it recovered tardily after 28 days, which associated with the degradation of extracellular vesicles and the saline solution cannot retention extracellular vesicles in the injured site after 28 days when injected into the *in vivo* environment. This phenomenon could be explained by the assay of retention and sustained extracellular vesicles release *in vivo*, indicating that extracellular vesicles could be intensely detected before 14 days and maintained about 28 days in extracellular vesicles treated group. While a remarkably longer and stronger signal of extracellular vesicles was detected at the injured site of spinal cord in the FE@EVs treated group which maintained the extracellular vesicles more than 56 days. Moreover, FE hydrogel group could also increase the motor functional recovery, while the BBB scores were no obviously statistical significance at first 21 days compared with SCI group. It can be explained that PCE polymer had the ability to maintain cell viability, which may improve the functional recovery after SCI [41]. The enhanced motor functional recovery by FE@EVs hydrogel was probably explained as follows. FE@EVs hydrogel could efficiently protect the bioactivity of extracellular vesicle and release it in long term in injured spinal cord, the adhesive ability could reduce the cavity area of spinal cord and prevent nerve retraction.

Both suppressing excessive reaction of inflammation and boosting remyelination are vital physiological process to regulate microenvironment in order to enhance function recovery after SCI [42,43]. Extensive experiments employing macrophage depletion or ablation models have demonstrated that macrophages performed neurotoxic

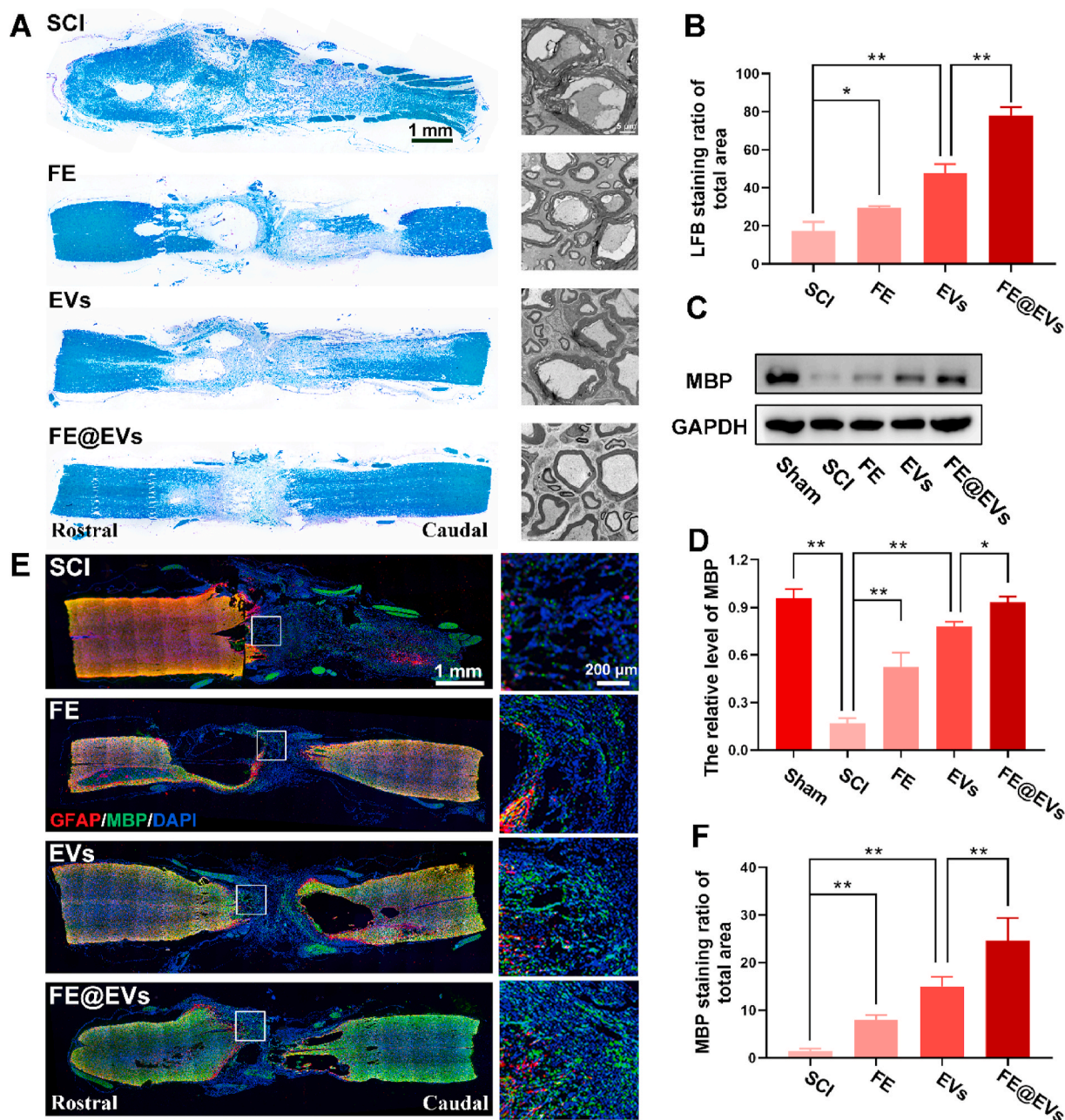


Fig. 6. FE@EVs hydrogel promotes remyelination. (A) LFB staining images of longitudinal sections and transmission electron microscope images of the myelin sheath in each group at 56 days postinjury. (B) Quantification of LFB positive area from A. (C, D) Representative western blotting images and quantification showing MBP protein levels in the lesion region. (E) MBP and GFAP immunolabeling of spinal cord sections at 56 days postinjury. (F) Quantification of MBP staining ratio of total spinal cord from E. $N \geq 4$ per group for histology analysis, $N \geq 4$ per group for western blot assay.

effect in central nervous system [43]. Contradictorily, macrophages or microglia also reported that it could enhance remyelination after spinal cord injury *via* driving oligodendrocyte differentiation and mediating tissue remodeling [44,45]. The antagonistic effects of macrophages were interpreted that the excessive activation of macrophages, and suppressing macrophages over-activation could promote injured spinal cord functional recovery [46]. Using liposomes encapsulated clodronate to ablate macrophages after CNS injury will significantly impair the clearance of myelin fragments and delay the process of remyelination [47], suggesting that none or excessive inflammatory response will restrain remyelination. In our study, FE@EVs could significantly enhance remyelination through reducing excessive activated macrophages and suppressing the *in vivo* and *in vitro* excessive inflammatory reaction which are likely associated with remyelination and help axonal

regeneration [48].

Furthermore, the scar tissue formation plays a vital role in limiting the axonal regeneration in injury microenvironment. As a healing response, scars can contain and isolate injured site spatially. However, scars fail to form an ideal tissue, which could replace the injured tissue structurally and functionally. Moreover, Nogo, MAGs and CSPGs those extracellular factors in scar tissues could suppress the restoration of function. Interestingly, the compensatory mechanism of neurons or glial cells, which could transform the scar into a more effective repair process would be inhibited by these factors [49,50]. Fibrotic scars are mainly composed of fibrocytes and extracellular factors. If the dura is damaged, fibroblasts, derived from meningeal cells or perivascular cells will proliferate and migrate into the injured area following contusion injury [51–55]. Our present data have showed that FE@EVs could remarkably

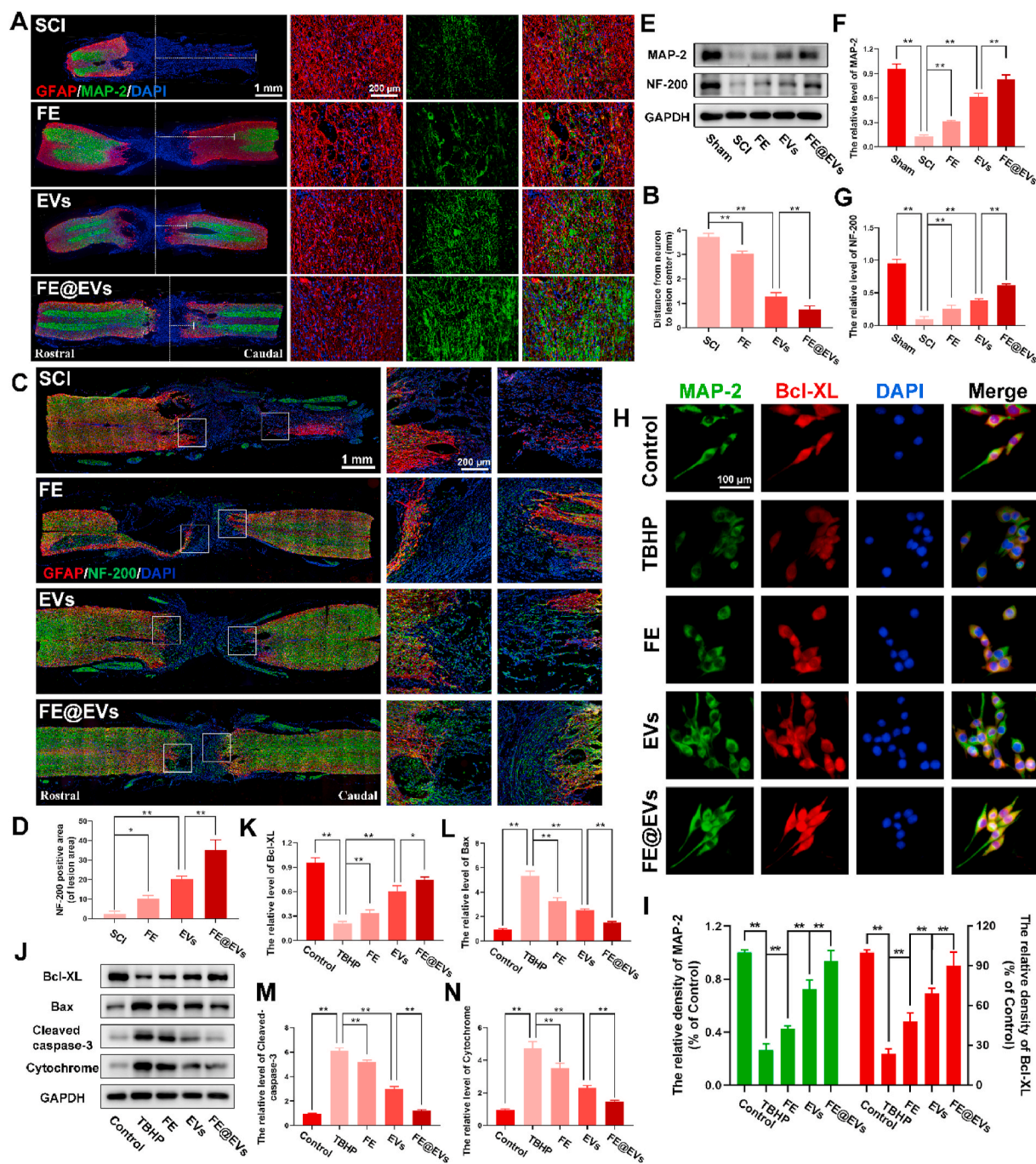


Fig. 7. FE@EVs hydrogel promotes axonal regeneration. (A) Images of whole spinal sections staining MAP-2 and GFAP from SCI and different treatment rats at 56 days postinjury, the white dotted line indicates center of lesion site. (B) Quantify the distance from the neuron to the center of the lesion. (C, D) Images and quantification of whole spinal sections staining NF-200 and GFAP from SCI and different treatment rats at 56 days postinjury. (E–G) Representative western blotting images and quantification showing MAP-2 and NF-200 protein levels in the lesion region. (H) MAP-2 and Bcl-XL immunolabeling in neurons. (I) Quantification of MAP-2 and Bcl-XL fluorescence intensity from H. (J–N) Representative western blotting images and quantification showing Bcl-XL, Bax, Cleaved-caspase-3 and Cytochrome protein levels in neurons. N ≥ 4 per group for histology analysis, N ≥ 4 per group for western blot assay.

suppress the fibrotic scar formation through attenuating fibroblast migration.

As understanding the pathophysiology of SCI, the protection of nerves and tissues promotes the development of nerve rehabilitation, plasticity, and axon regeneration. This is a potential and advanced method of treating spinal cord injury [56,57]. Our results indicated that FE@EVs hydrogel could perform an evident effect of attenuating tissue damage, while the FE or free extracellular vesicles group performed less tissue loss and neuronal damage. Protecting neurons ameliorated the

pathological morphology due to keeping the localized and sustained delivery of extracellular vesicles in the lesion area. For functional restoration after SCI, axonal regeneration is regard as an indispensable factor. Herein, FE@EVs significantly enhanced the axonal regeneration through activating the MAP-2 and neurofilament and suppressing the apoptosis of neurons [58], confirming the contribution of microenvironmental mitigation to axonal regeneration and neuron protection. In summary, our study shows that FE@EVs hydrogel is highly efficient and safe for nerve tissue repair after severe SCI.

4. Conclusions

We developed a safe and bioactive multifunctional citrate-based hydrogel therapeutic system with ultralong release of MSC-derived extracellular vesicle (FE@EVs) for efficiently enhancing spinal cord repair after SCI. The FE@EVs hydrogel showed excellent injectability, adhesive behavior, high extracellular vesicle loading/binding. The FE@EVs hydrogel effectively promoted the preservation and controlled release of extracellular vesicles up to 56 days on SCI site, exhibiting the capacity of microenvironment mitigation, including reactive fibrotic scar suppression, inflammatory reaction reduction, remyelination and axonal regeneration, which worked together and significantly enhanced tissue repair and motor functional restoration after SCI. FE@EVs hydrogel provides a promising extracellular vesicle-based delivery strategy for the efficient and biocompatible treatment of patients suffering from SCI.

5. Methods

5.1. Synthesis of PCE and FE hydrogels

The PCE polymer was synthesized by PCG prepolymer and branched polyethyleneimine (PEI 600) according to our previous report [28]. Briefly, the PCG prepolymer was synthesized using citric acid (CA), 1, 8-octanediol (OD) and polyethylene glycol (PEG) through a melt-derived polymerization. The PCE polymer was synthesized using branched polyethyleneimine (PEI 600) and PCG prepolymer via a typical catalytic reaction. The PCG prepolymer and PCE polymer were collected after purifying and freeze-drying. The temperature-responsive FE hydrogel was prepared using F127 (25 wt%) and PCE (0.01 wt%) by the simple blending. The ^1H NMR (Ascend 400 MHz, Bruker) and the FT-IR (NICOLET 6700, Thermo) were used to analyze the physicochemical structure of PCE polymer and FE hydrogel. Moreover, the SEM (GeminiSEM 500, Zeiss) was used to observe the morphology of FE hydrogel.

5.2. Multifunctional properties and rheological evaluations

The thermosensitivity of FE hydrogel was measured through observing the state of hydrogel at 4, 25, and 37 °C. The injectability of FE hydrogel was evaluated whether it can be extruded from the needle (0.9×38 mm). The self-healing ability of FE hydrogel was evaluated through observing the change of the two separated hydrogel state. The adhesive ability of FE hydrogel was evaluated through observing the adhesion effect of hydrogel to the skin and spinal cord. In addition, the rheological properties of FE hydrogel including the storage modulus (G'), loss modulus (G'') and viscosity were analyzed by the TA rheometer (DHR-2) under different temperature, oscillation strain or shear rate.

5.3. Animal model of SCI and treatment

This protocol was approved by Institutional Animal Care and Use Committee of Zhejiang University. Total 63 female rats (~230 g) were used as animal models to evaluate the efficacy of delivering extracellular vesicles within FE hydrogel for functional recovery after SCI. Rats were randomly divided into five groups: Sham (n = 12), SCI (n = 15), FE (n = 12), EVs (n = 12) and FE@EVs (n = 12). Moreover, in order to analyze the release of extracellular vesicle from hydrogel *in vivo*, another 8 rats were divided into two groups: EVs (n = 4) and FE@EVs (n = 4). Before surgery, animals were anesthetized with 1% (w/v) pentobarbital sodium (4 mL/kg, i.p.), shaved the back region, and aseptically prepared with 70% ethanol and betadine solution. In preparing spinal transection, the thoracic vertebra was exposed, the level of the T9–T11 vertebral column was resected by laminectomy and complete transection was made with a microscissor at the T10 segment of the spinal cord. To verify lesion completeness, lift the severed stump and pass the hook through the gap to ensure no residual fibers on the bottom and lateral sides of the

canal. 10 μL of saline, FE hydrogel, free extracellular vesicles solution or FE@EVs hydrogel was orthotopically injected to the injured site immediately. Extracellular vesicles retention and release behavior in FE@EVs hydrogel.

The FE@EVs hydrogel was obtained by mixing 1 μg extracellular vesicles with 100 μL FE hydrogel followed stirring at 4 °C. The extracellular vesicle release profile *in vitro* was detected by the Micro BCA protein assay kit. Briefly, 100 μL FE@EVs hydrogel prepared above was placed in the upper transwell chamber placed in a 24-well plate, while 100 μL PBS was added in the lower chamber. At day 0, 7, 14, 21, 28, 35, 42, 49 and 56, 10 μL PBS was collected and added the same volume of fresh PBS. The content of released extracellular vesicles was detected by the BCA kit and the released percentage of extracellular vesicles was calculated.

To analyze the release of extracellular vesicle from hydrogel *in vivo*, After operation of rats, the free extracellular vesicles solution (containing 100 ng extracellular vesicles labeled DiR diluted in PBS) or FE@EVs hydrogel (containing 100 ng extracellular vesicles labeled DiR) was orthotopically injected to the injured site (T10 complete transection of the spinal cord). Briefly, DiR (Thermo Fisher Scientific, USA, D12731) was added in extracellular vesicles solution at the concentration of 1:400 for 30 min followed by ultra-centrifuging at 100,000 g for 90 min to purify extracellular vesicles *via* removing redundant dye. The near-IR fluorescence images *in vivo* were observed using the IVIS Spectrum System (Perkin Elmer) once a week after SCI until 56 days postinjury with a 748 nm excitation wavelength and a 780 nm filter to quantify the radial efficiency. After 56 days postinjury, a lethal dose of pentobarbital sodium was applied to anaesthetize. Then animals were perfused with saline followed by 4% paraformaldehyde transcardially. Major organ samples, including spinal cord, heart, liver, spleen, lung, and kidney, were prepared to detect the fluorescent distribution *ex vivo*, followed by quantifying the radial efficiency.

5.4. Functional behavior evaluation

The Basso-Beattie-Bresnahan (BBB) motor functional score was performed to evaluate the mobility of posterior limbs after SCI. In short, the BBB score ranges from 0 (severe neurological deficits) to 21 (normal performance) points based on walking capacity, the movement and coordination of posterior limb joints. At a specific point in time, each rat was placed in an open field and record the BBB score by three independent observers who blinded to group identity last 5 min. Footprint analysis was assessed by coating fore limbs and posterior limbs with different colors (red for fore limbs and blue for posterior limbs). Subsequently, the animals were allowed to walk on a narrow pipeline which covered a straight strip of white paper. Finally, the white papers with footprints were scanned to be digitized images. The outcome measures were obtained by three independent examiners who were blinded to the experimental conditions.

5.5. Cell culture and drug treatment

HAPI microglial cells and PC12 were purchased from Cell Biology (Shanghai, China), L929 fibroblast cell line was purchased from iCell Bioscience Inc (Shanghai, China). Cells were cultured in high glucose DMEM medium (Sigma-Aldrich, USA) containing 10% FBS, 1% penicillin and streptomycin under appropriate conditions in a humidified incubator with 5% CO₂ at 37 °C. HAPI cells were reseeded in 12-well plates supplemented with or without 10 $\mu\text{g}/\text{mL}$ Lipopolysaccharide (LPS, Sigma-Aldrich, USA) for 48 h. Re-plate PC12 cells and culture in 12-well plates with or without 100 μM TBHP (Tert-butyl hydroperoxide, Sigma-Aldrich, USA) for 12 h. Then, transwell co-culture system (pore size: 8 μm , Corning, USA) was used to evaluate the effect of hydrogels. Briefly, PC12 or HAPI cells was seeded in the lower chamber for completely adhesion, then 100 μL hydrogels were added into the upper chamber and co-incubated with PC12 or HAPI cells. After that, cells

were used for western blot or prepared for immunofluorescent staining. The migratory activity of fibroblasts was investigated by a wound scratch assay and a transwell system. Fibroblast cells were reseeded into a 12-well plate and incubated for 24 h. Then, a straight wound area was created by a 200 μ L pipette tip in the fibroblast monolayer, followed by 100 μ L hydrogels (FE or FE@EVs) or free extracellular vesicles solution was added into the transwell inserts. Moreover, in order to analyze the migration abilities, fibroblasts were reseeded into the transwell inserts for fully adhesion and then 800 μ L hydrogels (FE or FE@EVs) or free extracellular vesicles solution were added into the lower chamber. Wound scratch and transwell images were observed and pictured at 0, 12, 24, 36 and 48 h under inverted microscope (Olympus, Tokyo, Japan), and 5 random fields of wound scratch and transwell images were captured and counted for statistical analysis.

5.6. Statistical analysis

Statistical significance ($*P < 0.05$ or $**P < 0.01$) was determined using one or two-way analysis of variance (ANOVA) with Tukey's post hoc testing (Prism 8.0, GraphPad Software). All data from three individual experiments and presented as means \pm standard deviation.

CRediT authorship contribution statement

Chenggui Wang: Conceptualization, Methodology, Formal analysis, Investigation, Writing - original draft. **Min Wang:** Conceptualization, Methodology, Formal analysis, Investigation, Writing - original draft. **Kaishun Xia:** Methodology, Formal analysis. **Jingkai Wang:** Supervision, Writing - review & editing. **Feng Cheng:** Formal analysis. **Kesi Shi:** Conceptualization, Supervision. **Liwei Ying:** Formal analysis. **Chao Yu:** Conceptualization, Supervision. **Haibin Xu:** Supervision, Writing - review & editing. **Shining Xiao:** Methodology. **Chengzhen Liang:** Conceptualization, Supervision. **Fangcai Li:** Conceptualization. **Bo Lei:** Supervision, Funding acquisition. **Qixin Chen:** Supervision, Funding acquisition.

Declaration of competing interest

The authors declare no competing financial interest.

Acknowledgments

This work was supported by National Natural Science Foundation of China (Grant No. 51872224, 81772379, 81972096 and 81902238), Zhejiang Province Health Foundation, China (Grant No. 2018KY092, WKJ-ZJ-1903), Nature Science Foundation of Zhejiang Province, China (Grant No. LQ18H060003).

Appendix A. Supplementary data

Supplementary data to this article can be found online at <https://doi.org/10.1016/j.bioactmat.2021.01.029>.

References

- [1] S.R. Andresen, F. Biering-Sørensen, E.M. Hagen, J.F. Nielsen, F.W. Bach, N. B. Finnerup, Pain, spasticity and quality of life in individuals with traumatic spinal cord injury in Denmark, *Spinal Cord* 54 (2016) 973–979.
- [2] C.S. Rivers, N. Fallah, V.K. Noonan, D.G. Whitehurst, C.E. Schwartz, J. A. Finkelstein, B.C. Craven, K. Ethans, C. O'Connell, B.C. Truchon, et al., Health conditions: effect on function, health-related quality of life, and life satisfaction after traumatic spinal cord injury. A prospective observational registry cohort study, *Arch. Phys. Med. Rehabil.* 99 (2018) 443–451.
- [3] S.V. Hiremath, N.S. Hogaboom, M.R. Roscher, L.A. Worobey, M.L. Oyster, M. L. Boninger, Longitudinal prediction of quality-of-life scores and locomotion in individuals with traumatic spinal cord injury, *Arch. Phys. Med. Rehabil.* 98 (2017) 2385–2392.
- [4] A.P. Tran, P.M. Warren, J. Silver, The Biology of regeneration failure and success after spinal cord injury, *Physiol. Rev.* 98 (2018) 881–917.
- [5] A.M. Rubiano, N. Carney, R. Chesnut, J.C. Puyana, Global neurotrauma research challenges and opportunities, *Nature* 527 (2015) S193–S197.
- [6] L. Li, B. Xiao, J. Mu, Y. Zhang, C. Zhang, H. Cao, R. Chen, H.K. Patra, B. Yang, S. Feng, et al., Viala Mno nanoparticle-dotted hydrogel promotes spinal cord repair regulating reactive oxygen species microenvironment and synergizing with mesenchymal stem cells, *ACS Nano* 13 (2019) 14283–14293.
- [7] L.M. Li, M. Han, X.C. Jiang, X.Z. Yin, F. Chen, T.Y. Zhang, H. Ren, J.W. Zhang, T. J. Hou, Z. Chen, et al., Peptide-tethered hydrogel scaffold promotes recovery from spinal cord transection via synergism with mesenchymal stem cells, *ACS Appl. Mater. Interfaces* 9 (2017) 3330–3342.
- [8] H. Ren, M. Han, J. Zhou, Z.F. Zheng, P. Lu, J.J. Wang, J.Q. Wang, Q.J. Mao, J. Q. Gao, H.W. Ouyang, Repair of spinal cord injury by inhibition of astrocyte growth and inflammatory factor synthesis through local delivery of flavopiridol in plga nanoparticles, *Biomaterials* 35 (2014) 6585–6594.
- [9] W. Liu, B. Xu, W. Xue, B. Yang, Y. Fan, B. Chen, Z. Xiao, X. Xue, Z. Sun, M. Shu, et al., A functional scaffold to promote the migration and neuronal differentiation of neural stem/progenitor cells for spinal cord injury repair, *Biomaterials* 243 (2020) 119941.
- [10] H. Kumamaru, K. Kadoya, A.F. Adler, Y. Takashima, L. Graham, G. Coppola, M. H. Tuszynski, Generation and post-injury integration of human spinal cord neural stem cells, *Nat. Methods* 15 (2018) 723–731.
- [11] Y.C. Hsu, Y.T. Wu, T.H. Yu, Y.H. Wei, Mitochondria in mesenchymal stem cell Biology and cell therapy: from cellular differentiation to mitochondrial transfer, *Semin. Cell Dev. Biol.* 52 (2016) 119–131.
- [12] K. Menezes, M.A. Nascimento, J.P. Gonçalves, A.S. Cruz, D.V. Lopes, B. Curzio, M. Bonamino, J.R. de Menezes, R. Borojevic, M.I. Rossi, et al., Human mesenchymal cells from adipose tissue deposit laminin and promote regeneration of injured spinal cord in rats, *PLoS One* 9 (2014), e96020.
- [13] L. Tang, X. Lu, R. Zhu, T. Qian, Y. Tao, K. Li, J. Zheng, P. Zhao, S. Li, X. Wang, et al., Adipose-derived stem cells expressing the neurogenin-2 promote functional recovery after spinal cord injury in rat, *Cell. Mol. Neurobiol.* 36 (2016) 657–667.
- [14] L.B. Balsam, A.J. Wagers, J.L. Christensen, T. Kofidis, I.L. Weissman, R.C. Robbins, Haematopoietic stem cells adopt mature haematopoietic fates in ischaemic myocardium, *Nature* 428 (2004) 668–673.
- [15] T. Katsuda, N. Kosaka, F. Takeshita, T. Ochiya, The therapeutic potential of mesenchymal stem cell-derived extracellular vesicles, *Proteomics* 13 (2013) 1637–1653.
- [16] M.Z. Ratajczak, T. Jadczyk, D. Pędziwiatr, W. Wojakowski, New advances in stem cell research: practical implications for regenerative medicine, *Pol. Arch. Med. Wewn.* 124 (2014) 417–426.
- [17] T. Imai, Y. Takahashi, M. Nishikawa, K. Kato, M. Morishita, T. Yamashita, A. Matsumoto, C. Charoenviriyakul, Y. Takakura, Macrophage-dependent clearance of systemically administered B16bl6-derived exosomes from the blood circulation in mice, *J. Extracell. Vesicles* 4 (2015) 26238.
- [18] K.L. Lankford, E.J. Arroyo, K. Nazimek, K. Bryniarski, P.W. Askenase, J.D. Kocsis, Intravenously delivered mesenchymal stem cell-derived exosomes target M2-type macrophages in the injured spinal cord, *PLoS One* 13 (2018), e0190358.
- [19] J.H. Huang, X.M. Yin, Y. Xu, C.C. Xu, X. Lin, F.B. Ye, Y. Cao, F.Y. Lin, Systemic administration of exosomes released from mesenchymal stromal cells attenuates apoptosis, inflammation, and promotes angiogenesis after spinal cord injury in rats, *J. Neurotrauma* 34 (2017) 3388–3396.
- [20] G. Sun, G. Li, D. Li, W. Huang, R. Zhang, H. Zhang, Y. Duan, B. Wang, Hucmsc derived exosomes promote functional recovery in spinal cord injury mice via attenuating inflammation, *Mater. Sci. Eng. C Mater. Biol. Appl.* 89 (2018) 194–204.
- [21] C. Subra, K. Laulagnier, B. Perret, M. Record, Exosome lipidomics unravels lipid sorting at the level of multivesicular bodies, *Biochimie* 89 (2007) 205–212.
- [22] X. Xu, X. Xia, K. Zhang, A. Rai, Z. Li, P. Zhao, K. Wei, L. Zou, B. Yang, W.K. Wong, Bioadhesive hydrogels demonstrating pH-independent and ultrafast gelation promote gastric ulcer healing in pigs, *Sci. Transl. Med.* 12 (2020), eaba8014.
- [23] L. Li, B. Yan, J. Yang, L. Chen, H. Zeng, Novel mussel-inspired injectable self-healing hydrogel with anti-biofouling property, *Adv. Mater.* 27 (2015) 1294–1299.
- [24] M. Wang, C. Wang, M. Chen, Y. Xi, W. Cheng, C. Mao, T. Xu, X. Zhang, C. Lin, W. Gao, et al., Efficient angiogenesis-based diabetic wound healing/skin reconstruction through bioactive antibacterial adhesive ultraviolet shielding nanodressing with exosome release, *ACS Nano* 13 (2019) 10279–10293.
- [25] Q. Feng, J. Xu, K. Zhang, H. Yao, N. Zheng, L. Zheng, J. Wang, K. Wei, X. Xiao, L. Qin, et al., Dynamic and cell-infiltratable hydrogels as injectable carrier of therapeutic cells and drugs for treating challenging bone defects, *ACS Cent. Sci.* 5 (2019) 440–450.
- [26] M. Wang, Y. Guo, Y. Xue, W. Niu, M. Chen, P.X. Ma, B. Lei, Engineering multifunctional bioactive citric acid-based nanovectors for intrinsical targeted tumor imaging and specific sirna gene delivery in vitro/in vivo, *Biomaterials* 199 (2019) 10–21.
- [27] Y. Du, J. Ge, Y. Li, P.X. Ma, B. Lei, Biomimetic elastomeric, conductive and biodegradable polycitrate-based nanocomposites for guiding myogenic differentiation and skeletal muscle regeneration, *Biomaterials* 157 (2018) 40–50.
- [28] M. Wang, Y. Guo, M. Yu, P.X. Ma, C. Mao, B. Lei, Photoluminescent and biodegradable polycitrate-polyethylene glycol-polyethyleneimine polymers as highly biocompatible and efficient vectors for bioimaging-guided sirna and mirna delivery, *Acta Biomater.* 54 (2017) 69–80.
- [29] Y. Guo, M. Wang, J. Ge, W. Niu, M. Chen, W. Cheng, B. Lei, In vivo bioactive biodegradable polycitrate nanoclusters enhances the myoblast differentiation and skeletal muscle regeneration P38 mapk signaling pathway, *Bioactive Mater.* 5 (2020) 486–495.

- [30] G.D.J. Olivier, W.M. Van Balkom, M.S. Raymond, V.C.B. Carlijn, C.V. Marianne, Extracellular vesicles: potential roles in regenerative medicine, *Front. Immunol.* 5 (2014).
- [31] X. Wang, K. Cao, X. Sun, Y.X. Chen, Z.X. Duan, L. Sun, L. Guo, P. Bai, D.M. Sun, J. Q. Fan, Macrophages in spinal cord injury: phenotypic and functional change from exposure to myelin debris, *Glia* 63 (2015) 635–651.
- [32] Y. Zhu, C. Soderblom, V. Krishnan, J. Ashbaugh, J.R. Bethea, J.K. Lee, Hematogenous macrophage depletion reduces the fibrotic scar and increases axonal growth after spinal cord injury, *Neurobiol. Dis.* 74 (2015) 114–125.
- [33] Q. Wang, Y. He, Y. Zhao, H. Xie, Q. Lin, Z. He, X. Wang, J. Li, H. Zhang, C. Wang, et al., A thermosensitive heparin-polyoxamer hydrogel bridges afgf to treat spinal cord injury, *ACS Appl. Mater. Interfaces* 9 (2017) 6725–6745.
- [34] S. Bruno, C. Grange, F. Collino, M.C. Deregibus, V. Cantaluppi, L. Biancone, C. Tetta, G. Camussi, Microvesicles derived from mesenchymal stem cells enhance survival in a lethal model of acute kidney injury, *PLoS One* 7 (2012), e33115.
- [35] L. Wang, S. Pei, L. Han, B. Guo, Y. Li, R. Duan, Y. Yao, B. Xue, X. Chen, Y. Jia, Mesenchymal stem cell-derived exosomes reduce A1 astrocytes via downregulation of phosphorylated nfkb P65 subunit in spinal cord injury, *Cell. Physiol. Biochem. : Int. J. Exp. Cell. Physiol. Biochem. Pharmacol.* 50 (2018) 1535–1559.
- [36] Y. Lu, Y. Zhou, R. Zhang, L. Wen, K. Wu, Y. Li, Y. Yao, R. Duan, Y. Jia, Bone mesenchymal stem cell-derived extracellular vesicles promote recovery following spinal cord injury via improvement of the integrity of the blood-spinal cord barrier, *Front. Neurosci.* 13 (2019) 209.
- [37] D.J. Allison, A. Thomas, K. Beaudry, D.S. Ditor, Targeting inflammation as a treatment modality for neuropathic pain in spinal cord injury: a randomized clinical trial, *J. Neuroinflammation* 13 (2016) 152.
- [38] S. Kawabata, M. Takano, Y. Numasawa-Kuroiwa, G. Itakura, Y. Kobayashi, Y. Nishiyama, K. Sugai, S. Nishimura, H. Iwai, M. Isoda, et al., Grafted human ips cell-derived oligodendrocyte precursor cells contribute to robust remyelination of demyelinated axons after spinal cord injury, *Stem Cell Rep.* 6 (2016) 1–8.
- [39] J. Ruschel, F. Hellal, K.C. Flynn, S. Dupraz, D.A. Elliott, A. Tedeschi, M. Bates, C. Sliwinski, G. Brook, K. Dobrindt, et al., Systemic administration of epothilone B promotes axon regeneration after spinal cord injury, *Science* 348 (2015) 347–352.
- [40] X.J. Wang, C.H. Peng, S. Zhang, X.L. Xu, G.F. Shu, J. Qi, Y.F. Zhu, D.M. Xu, X. Q. Kang, K.J. Lu, et al., Polysialic-acid-based micelles promote neural regeneration in spinal cord injury therapy, *Nano Lett.* 19 (2019) 829–838.
- [41] Y. Du, J. Ge, Y. Li, P.X. Ma, B. Lei, Biomimetic elastomeric, conductive and biodegradable polycitrate-based nanocomposites for guiding myogenic differentiation and skeletal muscle regeneration, *Biomaterials* 157 (2018) 40–50.
- [42] K. Bartus, E.R. Burnside, J. Galino, N.D. James, D.L.H. Bennett, E.J. Bradbury, ErbB receptor signaling directly controls oligodendrocyte progenitor cell transformation and spontaneous remyelination after spinal cord injury, *Glia* 67 (2019) 1036–1046.
- [43] Y.S. Lee, L.H. Funk, J.K. Lee, M.B. Bunge, Macrophage depletion and schwann cell transplantation reduce cyst size after rat contusive spinal cord injury, *Neural Regen. Res.* 13 (2018) 684–691.
- [44] A.D. Greenhalgh, J.G. Zarruk, L.M. Healy, S.J. Baskar Jesudasan, P. Jhelum, C. K. Salmon, A. Formanek, M.V. Russo, J.P. Antel, D.B. McGavern, et al., Peripherally derived macrophages modulate microglial function to reduce inflammation after cns injury, *PLoS Biol.* 16 (2018), e2005264.
- [45] V.E. Miron, A. Boyd, J.W. Zhao, T.J. Yuen, J.M. Ruckh, J.L. Shadrach, P. van Wijngaarden, A.J. Wagers, A. Williams, R.J.M. Franklin, et al., M2 microglia and macrophages drive oligodendrocyte differentiation during cns remyelination, *Nat. Neurosci.* 16 (2013) 1211–1218.
- [46] C. Wang, Q. Wang, Y. Lou, J. Xu, Z. Feng, Y. Chen, Q. Tang, G. Zheng, Z. Zhang, Y. Wu, et al., Salidroside attenuates neuroinflammation and improves functional recovery after spinal cord injury through microglia polarization regulation, *J. Cell Mol. Med.* 22 (2018) 1148–1166.
- [47] M.R. Kotter, A. Setzu, F.J. Sim, N.V. Rooijen, R.J. Franklin, Macrophage depletion impairs oligodendrocyte remyelination following lysocleithin-induced demyelination, *Glia* 35 (2001) 204–212.
- [48] J. Silver, E.S. Martin, G.P. Phillip, Central nervous system regenerative failure: role of oligodendrocytes, astrocytes, and microglia, *Cold Spring Harb. Perspect. Biol.* 7 (2015) a020602.
- [49] D.G. Andrew, G.P. Phillip, Extracellular matrix regulation of inflammation in the healthy and injured spinal cord, *Exp. Neurol.* 258 (2014) 24–34.
- [50] M.L. Condic, P.C. Letourneau, Ligand-induced changes in integrin expression regulate neuronal adhesion and neurite outgrowth, *Nature* 389 (1997) 852–856.
- [51] J.W. Fawcett, M.E. Schwab, L. Montani, N. Brazda, H.W. Müller, Defeating inhibition of regeneration by scar and myelin components, *Handb. Clin. Neurol.* 109 (2012) 503–522.
- [52] N. Klapka, H.W. Müller, Collagen matrix in spinal cord injury, *J. Neurotrauma* 23 (2006) 422–435.
- [53] C. Soderblom, X. Luo, E. Blumenthal, E. Bray, K. Lyapichev, J. Ramos, V. Krishnan, C. Lai-Hsu, K.K. Park, P. Tsoulfas, et al., Perivascular fibroblasts form the fibrotic scar after contusive spinal cord injury, *J. Neurosci. : Off. J. Soc. Neurosci.* 33 (2013) 13882–13887.
- [54] M. Okada, O. Miyamoto, S. Shibuya, X. Zhang, T. Yamamoto, T. Itano, Expression and role of type I collagen in a rat spinal cord contusion injury model, *Neurosci. Res.* 58 (2007) 371–377.
- [55] J.G. Cooper, S.J. Jeong, T.L. McGuire, S. Sharma, W. Wang, S. Bhattacharyya, J. Varga, J.A. Kessler, Fibronectin eda forms the chronic fibrotic scar after contusive spinal cord injury, *Neurobiol. Dis.* 116 (2018) 60–68.
- [56] M.R. Leanne, S.R. Matt, J.B. Elizabeth, Restoring function after spinal cord injury: towards clinical translation of experimental strategies, *Lancet Neurol.* 13 (2014) 1241–1256.
- [57] R.W. Philip, N.M. Bogdan, D.S. Catherine, F.M. Christoph, M.S. Adrian, G. Oliver, K. Martin, M. Thomas, A recoverable state of axon injury persists for hours after spinal cord contusion in vivo, *Nat. Commun.* 5 (2014) 5683.
- [58] Y. Rong, W. Liu, C. Lv, J. Wang, Y. Luo, D. Jiang, L. Li, Z. Zhou, W. Zhou, Q. Li, et al., Neural stem cell small extracellular vesicle-based delivery of 14-3-3t reduces apoptosis and neuroinflammation following traumatic spinal cord injury by enhancing autophagy by targeting beclin-1, *Aging* 11 (2019) 7723–7745.